Proceedings of the 10th World Congress on Electrical Engineering and Computer Systems and Sciences (EECSS'24)
Barcelona, Spain - August 19 - 21, 2024
Paper No. EEE 112
DOI: 10.11159/eee24.112

Simulated Power Control Balancing for a Solar & Battery Microgrid System

James Vrtis[1], Dr. Ediz Polat[2]
[1]School of Electrical Engineering & Computer Science, University of North Dakota
Grand Forks, North Dakota, USA
James.Vrtis@ndus.edu, Ediz.Polat@ndus.edu
[2]School of Electrical Engineering & Computer Science, University of North Dakota
Grand Forks, North Dakota, USA

Abstract **-** This paper discusses an evaluation of multiple simulations to balance the solar and battery output power in a microgrid system. The microgrid battery system is connected in parallel to a photovoltaic power system and hydrogen electrolyzer. The battery output is controlled by developing a signal response from a solar power reference. The solar power reference utilized balances battery power output during periods of solar irradiance. There are three simulations conducted in this study which evaluate the effectiveness of delivering continuous power over a 72-hour time frame to a hydrogen electrolysis and storage system. The simulations integrate three different control signals and two different control systems. There are advantages and disadvantages to utilizing an n-D lookup table and digital control signal for battery control, and are outlined from the results of the simulations.

***Keywords*:** microgrid, battery management, CC-CV, control signal

1. Introduction

The model analyzed utilizes a Photovoltaics (PV) power and battery system to power an electrolyzer to produce hydrogen. The concept of the microgrid green hydrogen system revolves around an environmentally friendly process to produce and store energy without carbon-based fuels or energy sources. The advantage to generating hydrogen and storing it for later use is the process has the capability to produce energy for power plants or as an alternate fuel system for hydrogen powered vehicles. Additionally, hydrogen is used in industrialized processes such as refining petroleum, treating metals, producing fertilizer, and processing foods [1]. The produced hydrogen in this simulation is shared as a metric for evaluating the differences in system performance between balancing solar and battery power.

While this simulation primarily evaluates the advantage of utilizing different power controllers to balance battery and solar power, this concept may also be implemented in similar green hydrogen microgrid systems. When sizing and analyzing system performance for battery storage within grid applications, accurate measurements of State of Charge (SOC) are required for both controlling the battery and monitoring the Depth of Discharge (DOD). Balancing the battery power output is important because it there are many metrics which effect the performance and significance in battery sizing and control between the two components for a given load which include: SoC, DoD, Maximum Power Demand to Maximum Solar Power Output Ratio (MDMP), & Battery Energy Capacity to Solar Energy Capacity Ratio (BCSC) [2]. Other studies have focused on the importance of balancing battery charging in a renewable energy microgrid configuration and utilizing a smart energy system to balance battery and other renewable energy power. If the generation of photovoltaic is sufficient and the battery is charged above the minimum SoC limit, then the intelligent microgrid will send the surplus energy back to the external power grid [3].

2. System Configuration

The model analyzed utilizes solar panels, a battery system, digital signal control system, electrolyzer and hydrogen storage system. This analysis builds off of the existing MathWorks simulation titled the "*Green Hydrogen Microgrid* ©" [4]. Figure 1 shows a visual depiction of this diagram process. For this evaluation, the load demand is provided as the electrolysis subsystem.

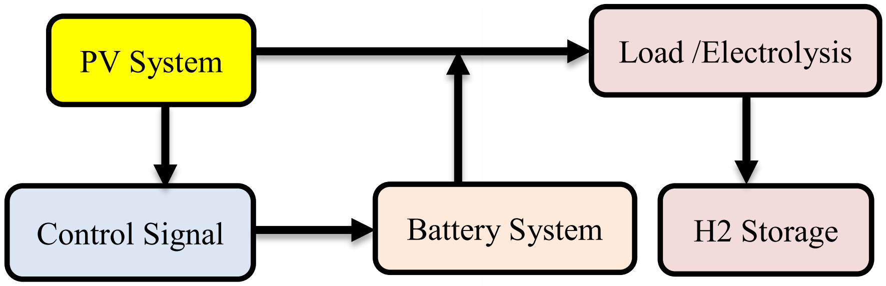

Fig. 1: Green hydrogen production and storage model.

The model analyzes how battery and PV power management are altered to efficiently manage the power supplied to the electrolyzer. The control signal and the battery control system and the two components configured and tested in the simulation to determine the effectiveness of balancing power sources. When the solar power is above or below an established parameter, then the battery system will activate to charge or discharge, dependent upon the designed control signal and battery control system. Balancing these two power sources is critical for efficiently providing enough power for a given period of time. This simulation aims to provide a constant source of power between the two power source components.

The "*Green Hydrogen Microgrid* ©" [4] model utilizes a current reference with a DC-DC converter; however, this project alters the cited model to evaluate battery power management with a battery Constant Current and Constant Voltage (CC-CV) controller control rather than the existing current reference DC-DC converter. The battery CC-CV controller is commonly used in distributed energy systems. The CC–CV mode used helps to keep the batteries SoC conditions for improving the reliability of the distributed power system. The CC-CV method is useful for maintaining the battery charge level and for maintaining the distributed power system network stability under transient load conditions [5]. The MathWorks Simulink battery CC-CV controller utilized provides multiple parameters for signal processing. The charging enabled parameter provides a boolean function to determine when the battery will be in a charging state or discharging state. This is a critical component to the system because the SoC is configured with this component to determine the cutoff for the battery charging state. Additionally, because this component is designed to provide a CC-CV, the current output and input for charging and discharging also configured within the simulation.

2.1 n-D Lookup Table

The "Green Hydrogen Microgrid" model [4] utilizes the technique of discharging the battery when the PV current begins to decline beyond a certain rate. As seen in Figure 2, that represents the operation of the microgrid during the maximum power generated by PV until the moment of power transition to battery power due to the reduction of solar power, which may be due to shading or because of the time of day. During the operation of maximum solar power, the loads must be connected and with the reduction of solar power these extra loads must be disconnected [6].

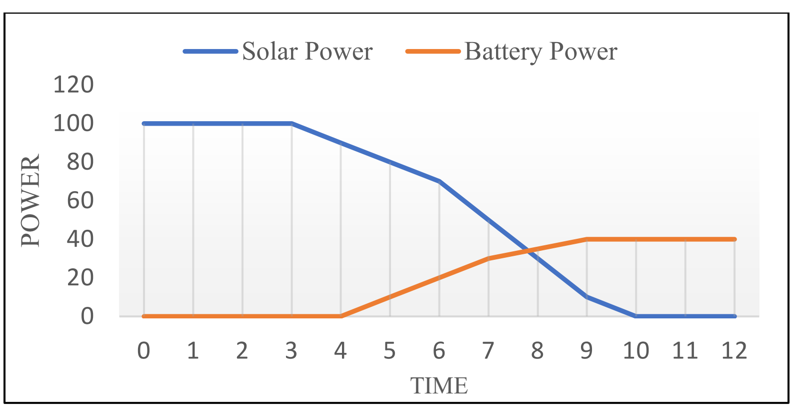

Fig. 2: Power balance between batter and PV system.

Furthermore, the original model utilizes a current n-D lookup table interpolation to optimize the battery power delivered to the circuit. The block maps inputs to an output value by looking up or interpolating a table of values you define with block parameters. Provided in Table 1 is an example of the how the existing model interpolated the current reference.

Table 1: Current reference look-up table.

	$Current_{RefSolar1}$	$Current_{RefSolar2}$	$Current_{RefSolarY}$
$Ahr_{Battery1}$	$Current_{Ref1} * n_1$	$Current_{Ref1} * n_2$	$Current_{Refn-2} * n_m$
$Ahr_{Battery2}$	$Current_{Ref2} * n_1$	$Current_{Ref2} * n_2$	$Current_{Refn-1} * n_m$
$Ahr_{BatteryZ}$	$Current_{Refz} * n_1$	$Current_{Refz} * n_2$	$Current_{Refz} * n_m$

2.2 Filtered Control Signal

The solar power generation over time was analyzed on the freqency spectrum of dBm over freqnecy. Similar studies have evaluated the differences in the frequency spectrum from the output power of PV system. Evaluating the power spectrum over the course of a year is prone to an array of dynamic solar irradiance profiles, which is why an appropriate filter type must be designed for the control signal. For example, a study conducted from the Oak Ridge National Laboratory found that the 12-month one-second time resolution solar power measurements collected from a 13-kW solar PV panel observed in the time-domain power profiles and a wide range of frequencies is observed in the frequency-domain profiles, ranging from a few hertz and fractions of Hertz (Hz), to multiple mHz, and to fractions of mHz [7]. Additionally, they found that about 98% of the PV energy is located in the low frequency band. The low frequency content corresponds to the daily solar power variations, which is commonly found in the parabola time profile shape. The medium frequency content comes from changes in solar irradiance due to moving clouds and other factors [7].

A High Pass Filter (HPF) is included to assist with controlling the threshold that will vary during intermittent weather conditions, whereas the Low Pass Filter (LPF) provides less harmonics with the solar irradiance profile. A sunny summer day may seldomly experience larger fluctuations in the high frequency band; whereas a typical cloudy winter day may experience less fluctuations in the high frequency band.

Signal control from the output of the filter is then passed through a buffer to perform frame-based processing over a specified sample period. The buffer frame size is determined by the desired frequency in battery power switching. The absolute value of the buffer is taken and summed to provide a signal over the specified sample period. The output of the summation then applies different logic conditions to determine a cutoff constant for the battery controller. The constant is variably determined by the desired output of the user. This does require the user to perform tuning control parameters to assess the various weather conditions that would affect power balancing performance conditions. For example, altering the buffer timeframe will affect the signal output from the cutoff constant determined [9].

There are 3 different simulations evaluated utilizing the cutoff constant. Figure 3 displays the signal flow for two of the simulations, which only utilize a HPF or LPF, and do not divide the signal from each other. Figure 4 provides the signal flow for utilizing both filters and dividing the signal before processing the cutoff value.

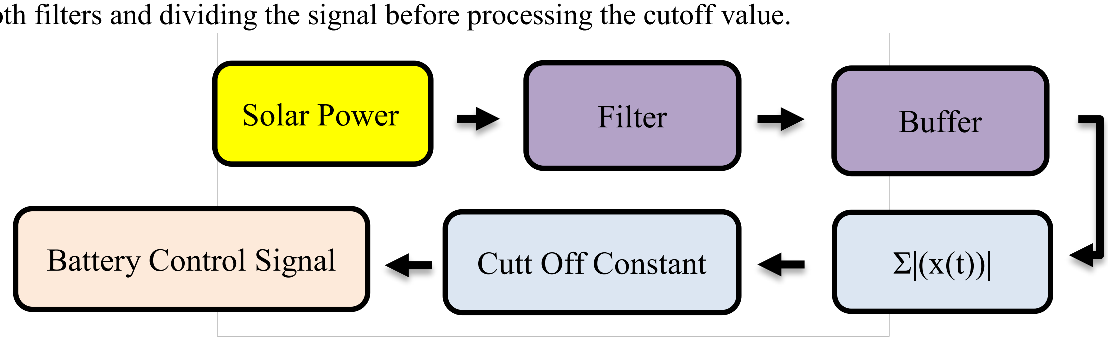

Fig. 3: Filtered digital signal control.

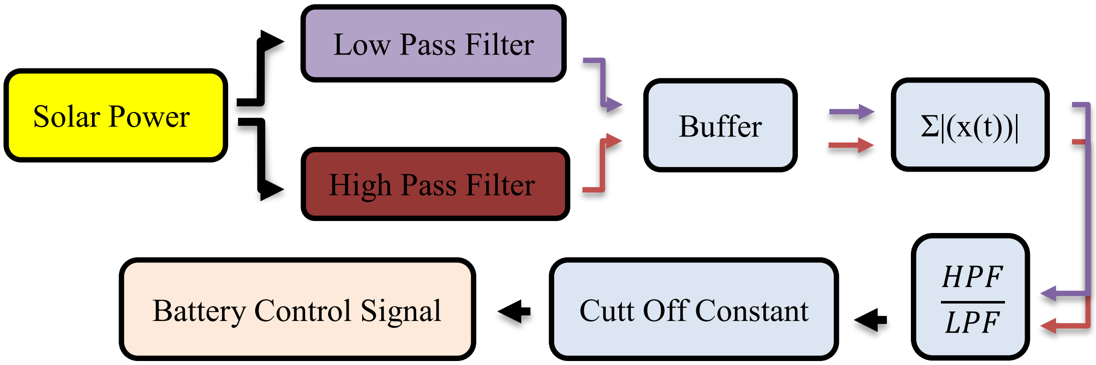

Fig. 4: LPF & HPF digital signal control.

3. System Modeling & Simulation

The experiment analyzed the implementation of three different scenarios: the n-D lookup table, HPF only, LPF only, and the combined HPF and LPF. The results display a comparison of the time profile of the power from each system in the microgrid, and the battery SoC and hydrogen produced at the end of the simulation.

3.1 n-D Lookup Table Simulation

Simulation results from the n-D lookup table and current reference-controlled DC-DC converter are provided in Figure 5, which display the power from each system component. The produced hydrogen and battery SoC at the end of the 3-day simulation was 40 kilograms (kg) and 87% respectively. The lookup n-D table values and solar power was altered from the MathWorks "*Green Hydrogen Microgrid* ©" [4].

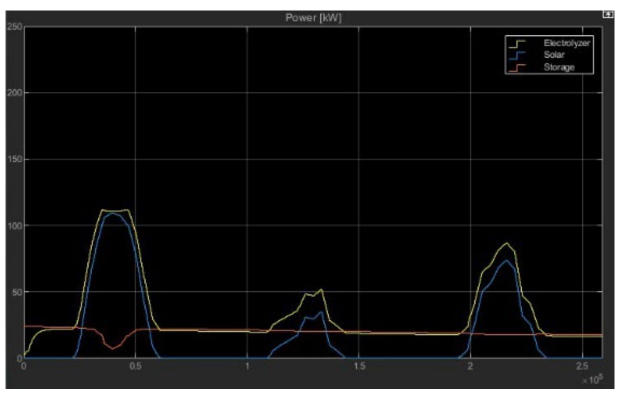

Fig. 5: Power over time supplied to the electrolyzer (yellow), power from the battery (orange), and power from the PV system (blue).

3.2 HPF Only

This simulation evaluated the results of only utilizing the HPF with a constant cutoff value to switch the binary signal. The simulation results from the HPF and battery CC-CV controller control are provided in Figures 6 and 7, which display the power from each system component and the filtered signal before being sent to the cutoff constant. At the end of the 3-day simulation, there was 33 kg of hydrogen produced and the SoC remained at 91%.

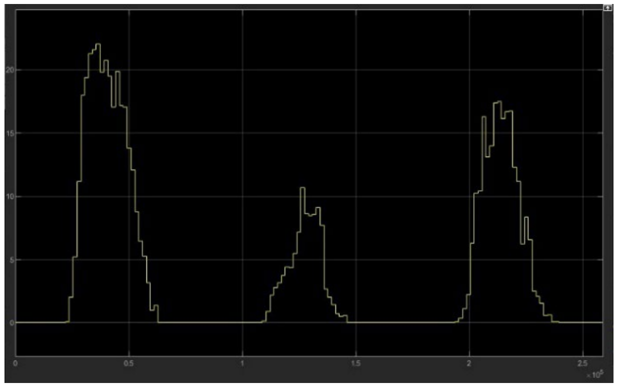

Fig. 6: HPF digital signal response after applying the absolute value and summing the results.

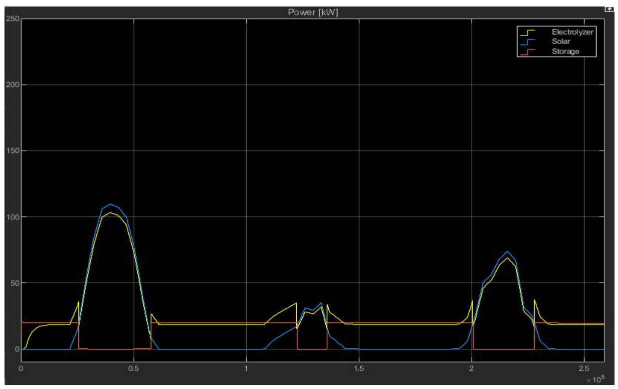

Fig. 7: Power over time supplied to the electrolyzer (yellow), power from the battery (orange), and power from the PV system (blue).

The results of the digital signal in Figure 9 display a similar trend to that shown in Figure 8 with the n-D lookup table. The results between each day are not normalized, but this system design does allow cutoff power during periods of high solar irradiance. Additionally, there is a constant battery power applied to the source and the output does allow for some overlap between the battery and solar power. The overlap prevents periods of low solar irradiance as the only source of power. The HPF filters through frequencies caused by cloudy and changing weather conditions. This is why the largest change in signal occurs during the increase and decrease of the bell curve.

3.3 LPF Only

This simulation evaluated the results of only utilizing the LPF with a constant cutoff value to switch the binary signal. The simulation results from the LPF and battery CC-CV controller control are provided in Figures 8 and 9, which display the power from each system component and the filtered signal before being sent to the cutoff constant. At the end of the 3-day simulation, there was 30 kg of hydrogen produced and the SoC remained at 93%.

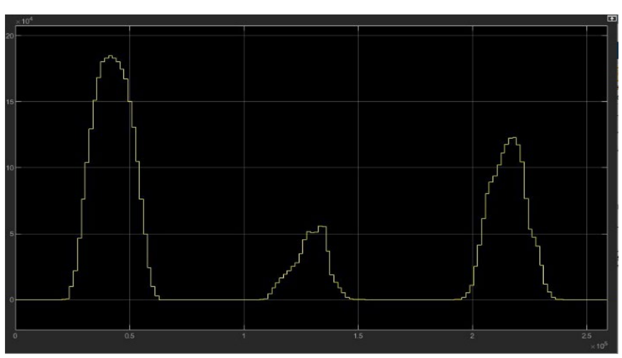

Fig. 8: LPF digital signal response after applying the absolute value and summing the results.

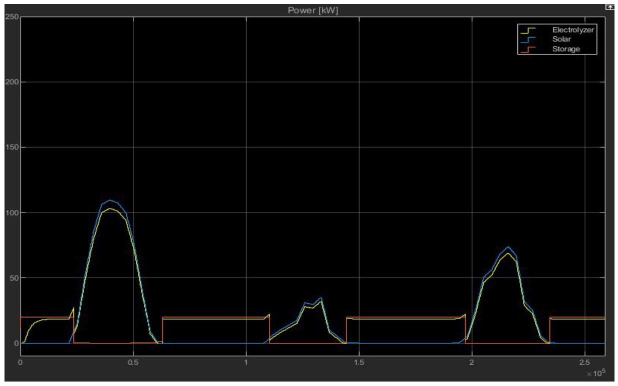

Fig. 9: Power over time supplied to the electrolyzer (yellow), power from the battery (orange), and power from the PV system (blue).

The digital signal shown in Figure 11 displays a trend similar to the HPF study and n-D Lookup table study. The cutoff used in this simulation allows for periods of low solar irradiance, which may not be ideal when there is a continuous source of power needed. As shown, there is a constant source of battery power applied to the source up until the solar irradiance begins to increase or decrease. Adjusting the cutoff would allow more overlap between solar and battery power, but this may cause strain to the battery and a high DoD during periods of low irradiance.

3.4 Combined HPF & LPF

This simulation evaluated the results of dividing the HPF over the LPF signal with a constant cutoff value to switch the binary signal. The simulation results from the battery CC-CV controller control are provided in Figures 10 and 11, which display the power supplied or absorbed from each system component and the filtered signal before being sent to the cutoff constant. At the end of the 3-day simulation, there was 30 kg of hydrogen produced and the SoC remained at 93%.

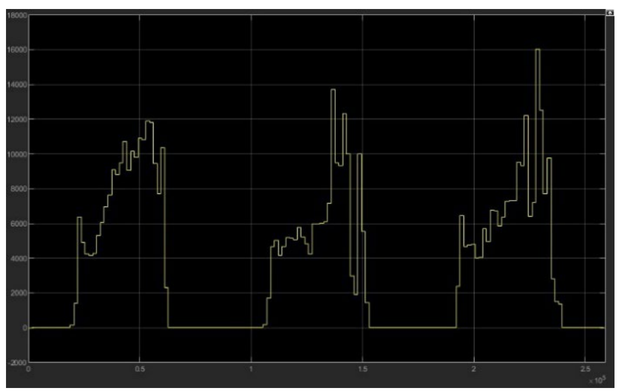

Fig. 10: Combined digital signal response after dividing the summation of the LPF and HPF signal.

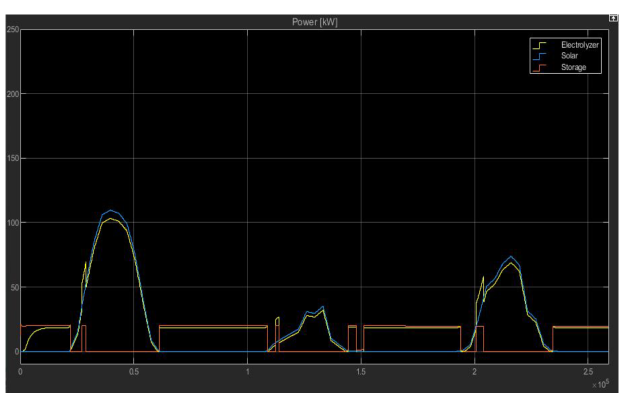

Fig. 11: Power over time supplied to the electrolyzer (yellow), power from the battery (orange), and power from the PV system (blue).

The digital signal shown in Figure 10 provides a comparatively normalized response between each of the 3 days. The downside with this response is that the cutoff constant is problematic to determine because the value chosen will affect overlap with battery and solar power at the start and end of the day since there is not a traditional bell curve shape to this signal. Adjusting the filter type and properties may improve the normalized signal to adjust for a different normalized response. Furthermore, there is periods of low power due to the battery cutoff at the start and end of the solar irradiance profile.

4.0 Conclusion

The concept of the existing DC-DC converter current reference simulation is more dynamic in some ways when controlling the output of the battery, because the lookup table provided a range of values to control the batteries output power dependent upon the battery SoC and solar current reference. However, those values are fixed and dependent on table parameters and may not necessarily account for seasonal changes throughout the year which could strain battery power for longer periods of time. If the battery is designed to always run at a given solar output, then the battery may never charge, or charge enough, from low solar irradiance profiles as a result of seasonal or weather changes.

Similar to the original simulation methodology, the digital control signal requires selecting the appropriate components and design for determining signal control parameters. Not only does the filter type matter, but there is an importance in determining the buffer frame size for frequency in power switching and determining the cutoff constant value. Additionally, because the output is controlled for a specified period of time, there are periods in this simulation where there is little battery or solar power output because the specified buffer period was too long. As shown in the simulation, there were brief periods of time where the battery cutoff when there were low periods of solar irradiance. However, this challenge could be overcome with better tuning of the parameters or integrating a neural network. Another benefit to the control signal design is that the HPF detects variations in weather conditions. If there is a sudden drop in solar power due to scattered clouds, those variations will be picked up by the filter and subsequently activate the battery.

In conclusion, the digital signal control managing power output supplied to the grid is able to effectively in balancing battery power supplied to the load. The digital signal control is an alternate method for controlling a battery power response to solar irradiance levels. Nevertheless, both models need adjustments to balance desired battery output dependent upon solar irradiance profiles levels and length of time needed to provide the desired battery powered response.

References

[1] U.S. Energy Information Administration, "Use of Hydrogen: Basics," U.S. Energy Information Administration, Washington, 2023.

[2] M. T. Lawder, V. Viswanathan and V. R. Subramanian, "Balancing autonomy and utilization of solar power and battery storage for demand based microgrids," Journal of Power Sources, 2015.

[3] W. Liu, N. Li, Z. Jiang, S. Wang, J. Han, X. Zhang and C. Liu, "Smart Micro-grid System with Wind/PV/Batter," Applied Energy Symposium and Forum 2018: Low carb, Shanghai, 2018.

[4] MathWorks Inc., "Green Hydrogen Microgrid," MathWorks Inc., 2021 - 2023.

[5] V. Virulkar, M. Aware and M. Kolhe, "Integrated battery controller for distributed energy system," Energy, vol. 36, no. 5, pp. 2392 - 2398, 2011.

[6] M. Mendes da Silva, C. Fleck dos Santos, A. M. S. S. Andrade and V. . M. Cleff, "Power Balance Control Strategy Battery Storage-PV," IEEE, 2021.

[7] M. Olama, J. Dong, . I. Sharma, Y. Xue and T. Kuruganti, "Frequency Analysis of Solar PV Power to Enable Optimal Building Load Control," MDPI, 2020.

[8] MathWorks, "Getting Started with Simulink for Signal Processing," MathWorks, 2023.